

NTP-driven translocation and regulation of downstream template opening by multi-subunit RNA polymerases¹

Zachary F. Burton, Michael Feig, Xue Q. Gong, Chunfen Zhang, Yuri A. Nediakov, and Yalin Xiong

Abstract: Multi-subunit RNA polymerases bind nucleotide triphosphate (NTP) substrates in the pretranslocated state and carry the dNMP–NTP base pair into the active site for phosphoryl transfer. NTP-driven translocation requires that NTP substrates enter the main-enzyme channel before loading into the active site. Based on this model, a new view of fidelity and efficiency of RNA synthesis is proposed. The model predicts that, during processive elongation, NTP-driven translocation is coupled to a protein conformational change that allows pyrophosphate release: coupling the end of one bond-addition cycle to substrate loading and translocation for the next. We present a detailed model of the RNA polymerase II elongation complex based on 2 low-affinity NTP binding sites located in the main-enzyme channel. This model posits that NTP substrates, elongation factors, and the conserved Rpb2 subunit fork loop 2 cooperate to regulate opening of the downstream transcription bubble.

Key words: RNA polymerase, NTP-driven translocation, transcriptional fidelity, transcriptional efficiency, α -amanitin.

Résumé : Les ARN polymérase à sous-unités multiples lient leurs substrats NTP dans un état de pré-translocation et apportent la paire de base dNMP–NTP au site actif pour le transfert du groupement phosphorylé. La translocation conduite par les NTP requiert que ces substrats NTP entrent dans un canal au sein de l'enzyme avant d'occuper le site actif. En se basant sur ce modèle, un nouveau point de vue de la fidélité et de l'efficacité de la synthèse de l'ARN est proposé. Ce modèle propose que durant l'élongation processive, la translocation conduite par les NTP est couplée à des changements de conformation de la protéine qui permettent le largage du pyrophosphate : le couplage de la fin d'un cycle d'addition d'une liaison au chargement du substrat et la translocation pour le prochain cycle. Nous présentons un modèle détaillé d'élongation du complexe de l'ARN polymérase II basé sur deux sites de liaison aux NTP de faible affinité localisés dans le canal principal de l'enzyme. Ce modèle avance que les substrats NTP, les facteurs d'élongation ainsi que la boucle 2 conservée de la sous-unité Rpb2 coopèrent pour réguler l'ouverture de la bulle de transcription en aval.

Mots clés : ARN polymérase, translocation conduite par les NTP, fidélité de la transcription, efficacité de la transcription, α -amanitine.

[Traduit par la Rédaction]

Translocation models

The virtue of transient-state (presteady-state) kinetic analysis is that functional dynamic changes in the elongation complex can be tracked through the formation of specific bonds on a millisecond time scale (Johnson 1992, 1995). As

such, the relationship between kinetic analyses and elongation mechanism becomes apparent. Based on transient-state studies of elongation catalyzed by human RNA polymerase II, we have proposed the nucleotide triphosphate (NTP)-driven translocation model (Nediakov et al. 2003a, 2003b; Zhang et al. 2003, 2005; Gong et al. 2004; Zhang and Burton

Received 6 February 2005. Revision received 29 March 2005. Accepted 30 March 2005. Published on the NRC Research Press Web site at <http://bcf.nrc.ca> on 23 July 2005.

Z.F. Burton,² M. Feig,³ X.Q. Gong, C. Zhang, Y.A. Nediakov, and Y. Xiong. Department of Biochemistry and Molecular Biology, Michigan State University, E. Lansing, MI 48824–1319, USA.

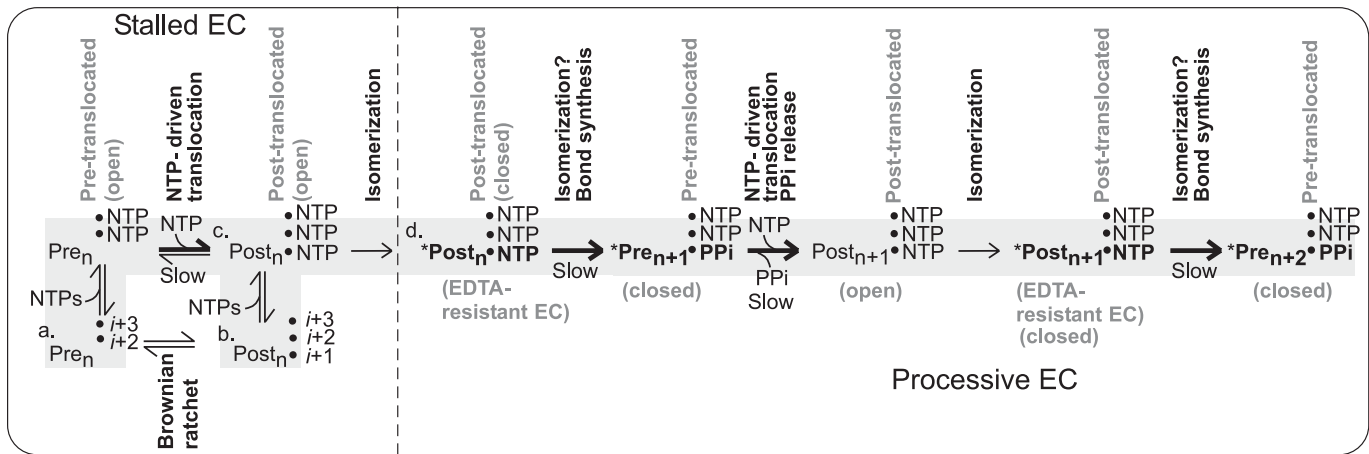
¹This paper is one of a selection of papers published in this Special Issue, entitled 26th International West Coast Chromatin and Chromosome Conference, and has undergone the Journal's usual peer review process.

²Corresponding author (e-mail: burton@msu.edu).

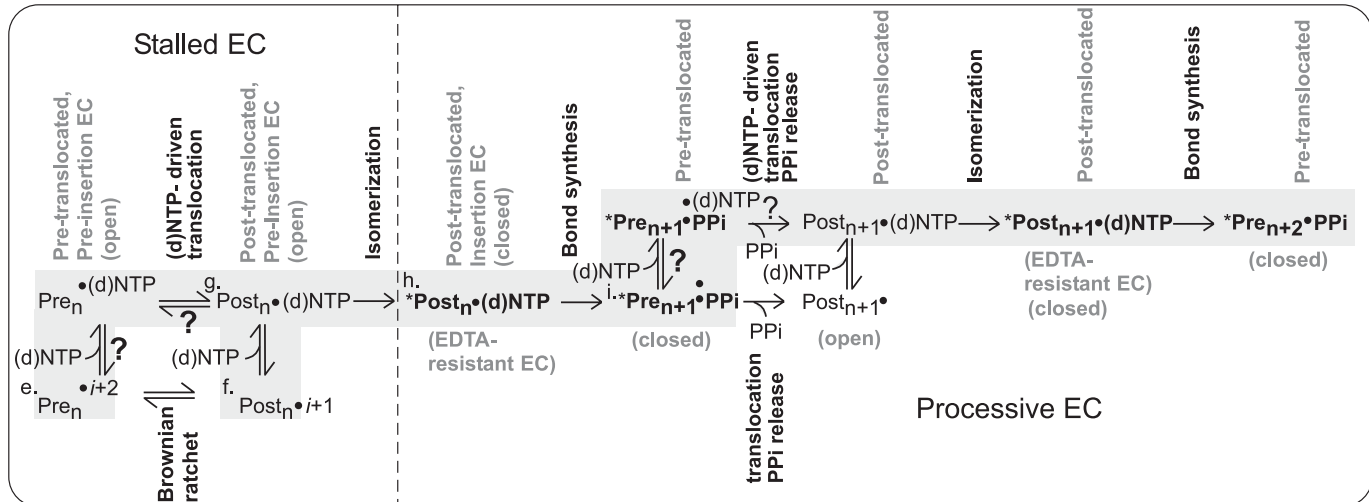
³Alternate address: Department of Chemistry, Michigan State University, E. Lansing, MI 48824, USA.

Fig. 1. Nucleotide triphosphate (NTP)-driven translocation for (A) multi-subunit RNA polymerases (RNAPs) and (d)NTP-driven translocation for (B) simple DNA (DNAPs) and RNA polymerases (proposed). Pretranslocation (pre) and post-translocation (post) elongation complexes (ECs) are indicated. Bold arrows indicate rate-limiting steps in the human RNA polymerase II mechanism. Rate-limiting steps may be different for some multi-subunit RNA polymerases. Bold type with an asterisk indicates an isomerized (closed) elongation complex. Elongation is shown for advancement from RNA or DNA length n to length $n+2$. Question marks indicate uncertainty in simple enzyme mechanisms (B). Continuous preloading of NTPs is indicated in the multi-subunit RNA polymerase mechanism (see subsequent figures). Elongation complexes that relate to published crystal structures are labeled: (a) Gnatt et al. 2001; (b) Westover et al. 2004a, 2004b; (c) Kettenberger et al. 2004; (d) Westover et al. 2004b; (e) Johnson et al. 2003; Johnson and Beese 2004; (f) Yin and Steitz 2002; Johnson et al. 2003; Johnson and Beese 2004; (g) Temiakov et al. 2004; (h) Yin and Steitz 2004; and (i) Yin and Steitz 2004. Active site ($i+1$) and downstream ($i+2$ and $i+3$) positions are indicated.

A Multi-subunit RNAPs



B Simple RNAPs + DNAPs



2004; Gong et al. 2005). Competing models to describe elongation and translocation include the allosteric model, posited by Erie and colleagues (Foster et al. 2001; Holmes and Erie 2003), and the thermal or Brownian-ratchet model, championed by Sousa, Nudler, and others (Guajardo and Sousa 1997; Oster 2002; Wang and Oster 2002; Sousa 2003, 2005; Landick 2004; Bar-Nahum et al. 2005). We find fault with these models, but describe the merits of disparate views. The purpose of this review is to consider NTP-driven translocation in the context of structural data and alternative models. Because much of the evidence for our model has

been published, we will concentrate on qualitative descriptions of our model and related models.

Rate-limiting steps during elongation

During processive RNA synthesis, human RNA polymerase II has 2 primary rate-limiting steps: NTP-driven translocation coupled to pyrophosphate release and phosphodiester bond synthesis (or a strongly coupled but unknown conformational change) (Fig. 1A) (Nedialkov et al. 2003a, 2003b; Zhang et al. 2003, 2005; Gong et al. 2004; Zhang

and Burton 2004). These 2 rate-limiting steps are sufficient to explain overall rates of RNA polymerase II elongation (15 to 30 nucleotides per second). NTP loading is rapid but is initially low-affinity, as expected for an interaction mediated primarily through base-pairing, recognition of the triphosphate (i.e., through basic side chain contacts), and scanning of the ribose ring (to exclude dNTP loading). For human RNA polymerase II, isomerization is rapid, followed by relatively slow phosphodiester-bond synthesis. During a primary isomerization step, the incoming substrate NTP-Mg²⁺ is tightened in the RNA polymerase II active site, where the metal is sequestered from chelation by EDTA (Zhang and Burton 2004; Zhang et al. 2005). Despite tight binding of the incoming NTP-Mg²⁺, subsequent phosphoryl transfer is delayed. This is a somewhat confusing result, because the phosphoryl transfer reaction is expected to proceed very rapidly (Patel et al. 1991). One way to explain this apparent contradiction is to speculate that, after the NTP-Mg²⁺ is initially tightened in the RNA polymerase II active site, the substrate must be further distorted (i.e., puckering the ribose sugar and (or) aligning the triphosphate) before bond formation can occur (Castro et al. 2005).

Interesting similarities have been observed in the kinetics of RNA polymerase II (12 subunits) and simpler DNA and RNA polymerases, which are generally single subunit enzymes and are not homologous to multi-subunit enzymes. For the RNA-dependent RNA polymerase of poliovirus, analyzed in the presence of Mn²⁺, isomerization is rapid, and is followed by rate-limiting bond formation (Arnold and Cameron 2004; Arnold et al. 2004; Castro et al. 2005). In this case, isomerization is defined by sequestration of NTP-Mn²⁺ in the active site, so that the metal is no longer available to react with EDTA as the reaction-quenching agent. On the other hand, with Mg²⁺ as the metal cofactor, for poliovirus RNA polymerase, isomerization (resistance to EDTA quench) is apparently coincident with bond formation (acid quench). This result indicates that, in the Mn²⁺-supported reaction, after initial tight sequestration of the NTP-Mn²⁺ in the active site, another isomerization step might be necessary to complete bond synthesis. Of significant interest is the startling similarity of the poliovirus RNA polymerase elongation kinetics in the presence of Mn²⁺ to the human RNA polymerase II elongation reaction in the presence of the physiological metal Mg²⁺.

NTP-driven translocation

Two relatively rapid kinetic phases are clearly resolved for human RNA polymerase II elongation from a stall position (Nedialkov et al. 2003a, 2003b; Zhang et al. 2003, 2005; Gong et al. 2004; Zhang and Burton 2004) (Fig. 1A). These phases have been interpreted as elongation from the pre- and post-translocation states of the elongation complex. As expected, elongation from the post-translocation state is much faster than from the pretranslocation state. Occupancy of the 2 phases is changed in the presence of different sets of elongation factors, showing that accessory factors shift RNA polymerase II between functional modes (translocation states), as expected. The pretranslocation state is highly sensitive to α -amanitin inhibition, but the post-translocation

state is resistant; the distinct rates of elongation clearly distinguish the 2 phases (Gong et al. 2004). The mushroom toxin α -amanitin has been shown to block translocation. Both pre- and post-translocation states are responsive to NTP substrates, showing that the pretranslocated elongation complex binds a templated NTP substrate.

The binding of an NTP to the pretranslocated elongation complex is consistent with the NTP-driven translocation model and the allosteric model, but not the Brownian-ratchet model. The Brownian-ratchet model has little meaning if the NTP substrate binds prior to translocation and drives translocation forward (Wang and Oster 2002; Landick 2004). The Brownian-ratchet mechanism requires that thermal motion drive translocation and that the NTP act as a pawl (as on a mechanical ratchet) to fix the elongation complex in the post-translocation state (Bar-Nahum et al. 2005; Sousa 2005). The observed binding of the substrate NTP to the pretranslocation state of the elongation complex converts the Brownian-ratchet model into the NTP-driven translocation model. The elongation mechanism for human RNA polymerase II, however, has characteristics of both NTP-driven translocation (the favored pathway) and a Brownian-ratchet (the default pathway in the absence of NTP substrates) (Fig. 1A). When NTPs are not present, the elongation complex fractionates into both the pre- and post-translocation states, so RNA polymerases can function as Brownian ratchets, at least in the absence of NTPs or during transcriptional stalling.

The allosteric model is based on millisecond-phase kinetic studies of *Escherichia coli* RNA polymerase elongation (Foster et al. 2001; Holmes and Erie 2003). The model describes an allosteric transition between an unactivated state and an activated state of the RNA polymerase elongation complex, apparently requiring multiple interactions with the next incoming NTP substrate. The difficulty with the allosteric model is that, because the allosteric site is templated, allostery appears to require 2 NTP substrates simultaneously base-paired to the same DNA template base. As far as we can determine, there is no satisfactory explanation for this conundrum. We do, however, support the following predictions of the allosteric model. First, an NTP substrate bound in the pretranslocation state acts as an allosteric effector to drive translocation forward from the unactivated state (pretranslocation state) to the activated state (post-translocation state) (Zhang and Burton 2004; Zhang et al. 2005). As far as we can discern, the allosteric model reduces to the NTP-driven translocation mechanism, and no other view of the allosteric model makes physical sense. Second, our laboratory has demonstrated other allosteric effects of the incoming NTP substrate during transfer from the pre- to the post-translocation positions (Gong et al. 2005). Specifically, the fate of a templated NTP tightened in the RNA polymerase II active site is linked to the presence of NTPs paired at the next 2 downstream template positions. Because these experiments demonstrate simultaneous occupancy of the pre- and post-translocation states of the elongation complex, they demonstrate the major tenet of the NTP-driven translocation model, which requires that both template positions be occupied by NTP substrates. So the allosteric model is verified

to this extent: the incoming NTP substrate acts in a manner similar to an allosteric effector to drive translocation forward.

Another prediction of our model is that, during processive RNA synthesis, NTP-driven translocation is coupled to pyrophosphate release from the previous bond-addition cycle (Zhang and Burton 2004; Zhang et al. 2005). We posit that, during processive synthesis, pyrophosphate remains locked in a tightened (closed) conformation of the elongation complex. For pyrophosphate to be released, the active site must first be relaxed to the open conformation. NTP-driven translocation induces the closed→open conformational change in the elongation complex that results in pyrophosphate release (Fig. 1A).

This feature of our model is demonstrated when human RNA polymerase II elongation in the presence of TFIIF is compared with TFIIF-mutant proteins defective in stimulating elongation (Zhang et al. 2005). We identified TFIIF-mutant proteins that fail to fully support NTP-driven translocation. As a result, the processive transition between phosphodiester bonds, which requires release of pyrophosphate, becomes very slow. Because bond completion (pyrophosphate release) relies on NTP-driven translocation, this step is highly dependent on the concentration of the incoming NTP. This NTP-driven step is facilitated by wild-type TFIIF. In the presence of the mutant TFIIF protein, RNA polymerase II escapes from a transcriptional stall by a mechanism that appears to be NTP-independent. Stalled RNA polymerase II lacks tightly bound pyrophosphate. Pyrophosphate release results in the acceleration of the NTP-independent translocation pathway, because relaxation of the active site during stalling frees the Brownian ratchet (Fig. 1A). During a processive transition, only the NTP-driven pathway is available until pyrophosphate can spontaneously be released, a slow process unless this step is facilitated by TFIIF and (or) the incoming NTP.

NTP loading into the RNA polymerase active site

Elongation complex structures have been published for yeast RNA polymerase II (Gnatt et al. 2001; Kettenberger et al. 2004; Westover et al. 2004a, 2004b) (Figs. 2–4), and these structures are consistent with the NTP-driven translocation model. These structures, however, indicate that the previously assumed route of NTP entry into the RNA polymerase active site, the secondary pore, is not the main route of NTP entry. The secondary pore presents a narrow channel with a highly negative electrostatic potential (Batada et al. 2004), so the pore does not appear to be a favorable NTP-loading route. Rather, the main entry port for NTP substrates must pass through the main enzyme channel. For a stalled elongation complex in the post-translocation state, the secondary pore is the likely route of NTP entry (Kettenberger et al. 2004; Westover et al. 2004a, 2004b). In the pretranslocation state, however, the DNA template base is single stranded and faces the main enzyme channel, not the secondary pore (Gnatt et al. 2001). To the pretranslocation state, therefore, the main enzyme channel is the likely route of NTP entry, and the secondary pore is excluded as a potential loading route. Kinetic studies demon-

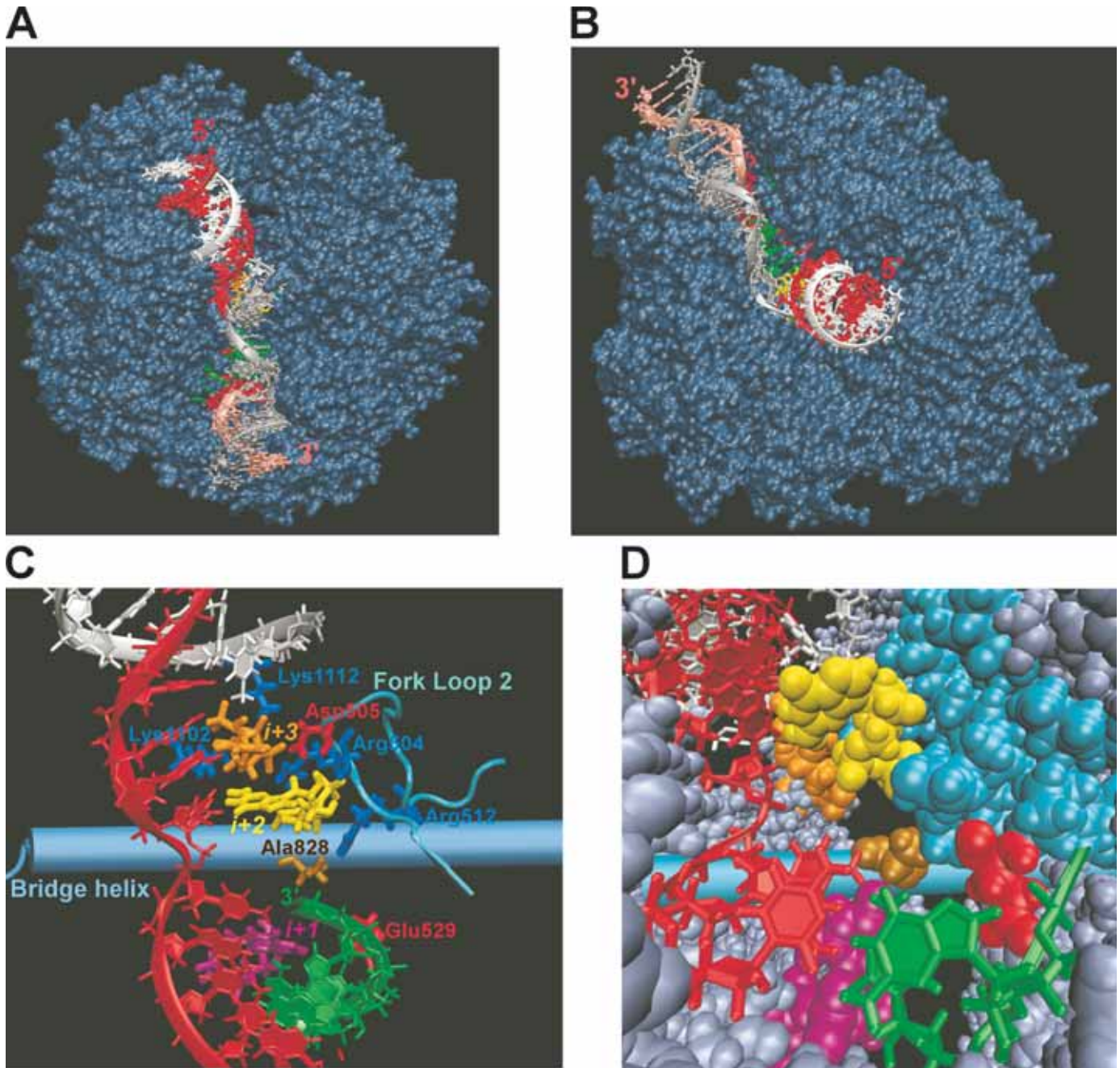
strate that the pretranslocation state of the elongation complex binds NTPs (Nedialkov et al. 2003a; Gong et al. 2004, 2005; Zhang and Burton 2004; Zhang et al. 2005). During processive synthesis, NTPs occupy the pretranslocation position, while the post-translocation position is occupied by the substrate NTP; this means that, under normal elongation conditions, NTPs enter the active site from the main enzyme channel. Only when the RNA polymerase stalls, releases pyrophosphate, and then translocates, can NTPs be loaded through the secondary pore, a situation that does not arise during processive synthesis (Fig. 1A). Sufficient space is available to load NTPs from the main channel into the RNA polymerase II active site (Fig. 2D).

What is the energetic driving force that propels the dNMP–NTP base pair to advance from the $i+2$ position to the $i+1$ active site (Fig. 3)? From observation of available elongation complex structures, there is no obvious answer to this question. We assume that the accurately paired NTP acts in a manner similar to an allosteric effector to induce a conformational change in RNA polymerase II that drives translocation of the RNA–DNA hybrid forward. Bending of the bridge α -helix (Gnatt et al. 2001), rearrangement of the trigger loop (Vassilyev et al. 2002; Bar-Nahum et al. 2005), and movement of other mobile protein switches (Holmes and Erie 2003) may be involved in the NTP-driven translocation mechanism.

Available elongation complex structures of yeast RNA polymerase II present different views of the number of single-stranded DNA template bases available for NTP pairing in the main enzyme channel. A structure from the Kornberg laboratory indicates at least 3 main channel single-stranded template bases ($i+2$, $i+3$, and $i+4$; $i+1$ represents the position of an NTP in the active site poised for bond formation) (Gnatt et al. 2001). More recent structures from the same researchers have shown a similar position for bubble melting ($i+4$ is unpaired). The nontemplate DNA strand in these structures, however, lacked bases $i+2$ and $i+3$, inhibiting its capacity to anneal (Westover et al. 2004b). The structure from the Cramer laboratory shows that the downstream bubble can close, leaving (at most) a single base ($i+2$) unpaired in the main enzyme channel (Kettenberger et al. 2004). The Cramer structure is not informative about the unpaired $i+2$ base, because the $i+2$ base was selected to be unpaired. To support the NTP-driven translocation mechanism, a single unpaired DNA base ($i+2$) in the main-enzyme channel is minimally sufficient (Nedialkov et al. 2003a; Zhang and Burton 2004), and none of the available structures contradict this requirement.

Based on experiments with human RNA polymerase II, however, at least 3 DNA bases appear to be simultaneously available for pairing NTP substrates ($i+1$, $i+2$, and $i+3$), (Gong et al. 2005; Fig. 2). This result is in apparent contradiction to the Cramer structure, but it appears to be consistent with the Kornberg structures. We therefore propose that the Cramer elongation complex suffers downstream bubble collapse. The Cramer elongation complex has a 7- rather than an 8-base-pair RNA–DNA hybrid (Kireeva et al. 2000; Gnatt et al. 2001), and the crystal is badly disordered upon addition of a substrate analogue (GMPcPP), which fails to load accurately into the catalytic site (Kettenberger et al.

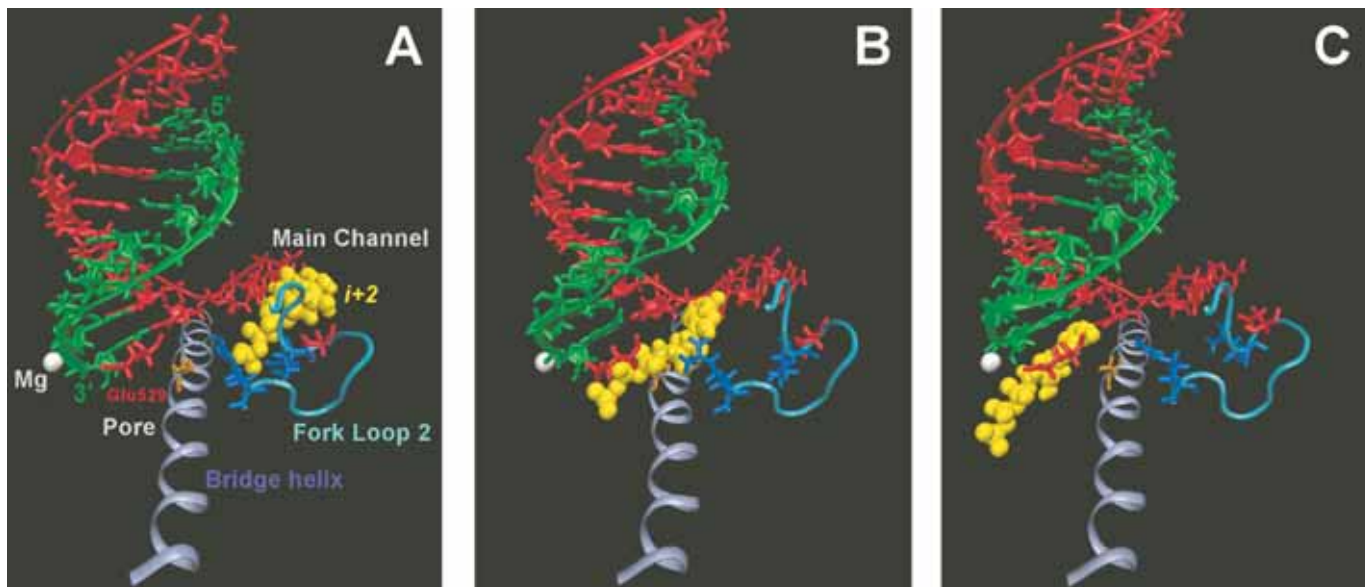
Fig. 2. Three NTP binding sites in RNA polymerase II. (A and B) Two views of the yeast RNA polymerase II elongation complex structure (Gnatt et al. 2001; Westover et al. 2004b). (C and D) Simplified views of main channel ($i+2$ and $i+3$) and active site ($i+1$) NTP-loading sites. (C) Stick figures with labeled amino acids thought to be involved in NTP binding and NTP-driven translocation. Fork loop 2 (Rpb2 region Asn499 to His515) is a light blue ribbon. (D) Space-filling representation, indicating the open space between the $i+2$ and $i+1$ sites. Minor movements of Rpb2 fork loop 2 (light blue; amino acids Rpb2 500–540 are shown) is necessary for NTP passage from $i+2$ to $i+1$. DNA-template strand is red (from crystal structures) or pink (modeled, upstream DNA). The nontemplate strand is white (from crystal structures) or silver (modeled, bubble and upstream DNA). The modeled open complex is 18 bases. RNA is green. The bridge α -helix is a blue cylinder. The $i+1$ (active site) (purple), $i+2$ (yellow), and $i+3$ (orange) NTPs are indicated. Rpb2 Arg504, Rpb2 Arg512, Rpb1 Lys1102, and Rpb1 Lys1112 (blue) are indicated. Rpb2 Asp505 and Rpb2 Glu529 (red) and Rpb1 Ala828 (brown) are shown.



2004). In the Cramer structure, the $i+2$, $i+3$, and $i+4$ DNA base pairs are strained, as if they are likely to separate in a more favorable conformation of the elongation complex. There is no clear demonstration that the Cramer structure is

highly active, leading us to wonder whether the crystals would disorder upon addition of a natural GTP substrate, as they appear to do attempting to load the GMPCPP analogue. The Cramer elongation complex does not represent the only

Fig. 3. NTP-driven translocation by human RNA polymerase II. (A) Pretranslocation elongation complex. Colors are the same as those indicated in Fig. 2. (B) Translocation intermediate. (C) Post-translocation elongation complex. Space is available to load an NTP (yellow) from the $i+2$ main-channel site to the $i+1$ active site. An active site, Mg^{2+} (white), is shown.



configuration of the downstream elongation bubble; the Kornberg structures, with 3 unpaired DNA bases in the main enzyme channel ($i+2$, $i+3$, and $i+4$) (Gnatt et al. 2001; Westover et al. 2004b), appear to be more accurate portrayals of a functional RNA polymerase II elongation complex. An NTP substrate loaded in the active site ($i+1$) senses the presence of at least 2 downstream templated NTP bases ($i+2$ and $i+3$), using verified and functional human RNA polymerase II elongation complexes (Gong et al. 2005). Because ours is a kinetic experiment, we do not know the structural positions occupied by incoming NTPs, but we have modeled possible positions in Figs. 2C and 2D. Our experiments are done with human enzyme, and available crystal structures are of the yeast enzyme. It is possible that there are differences in the regulation of the downstream transcription bubble in different multi-subunit RNA polymerases, although we do not believe that this is the case for RNA polymerase II from different species. We guess that all multi-subunit RNA polymerases use similar NTP-driven translocation mechanisms (see supplementary text and figures for an evolutionary comparison⁴).

A structural model for NTP-driven translocation

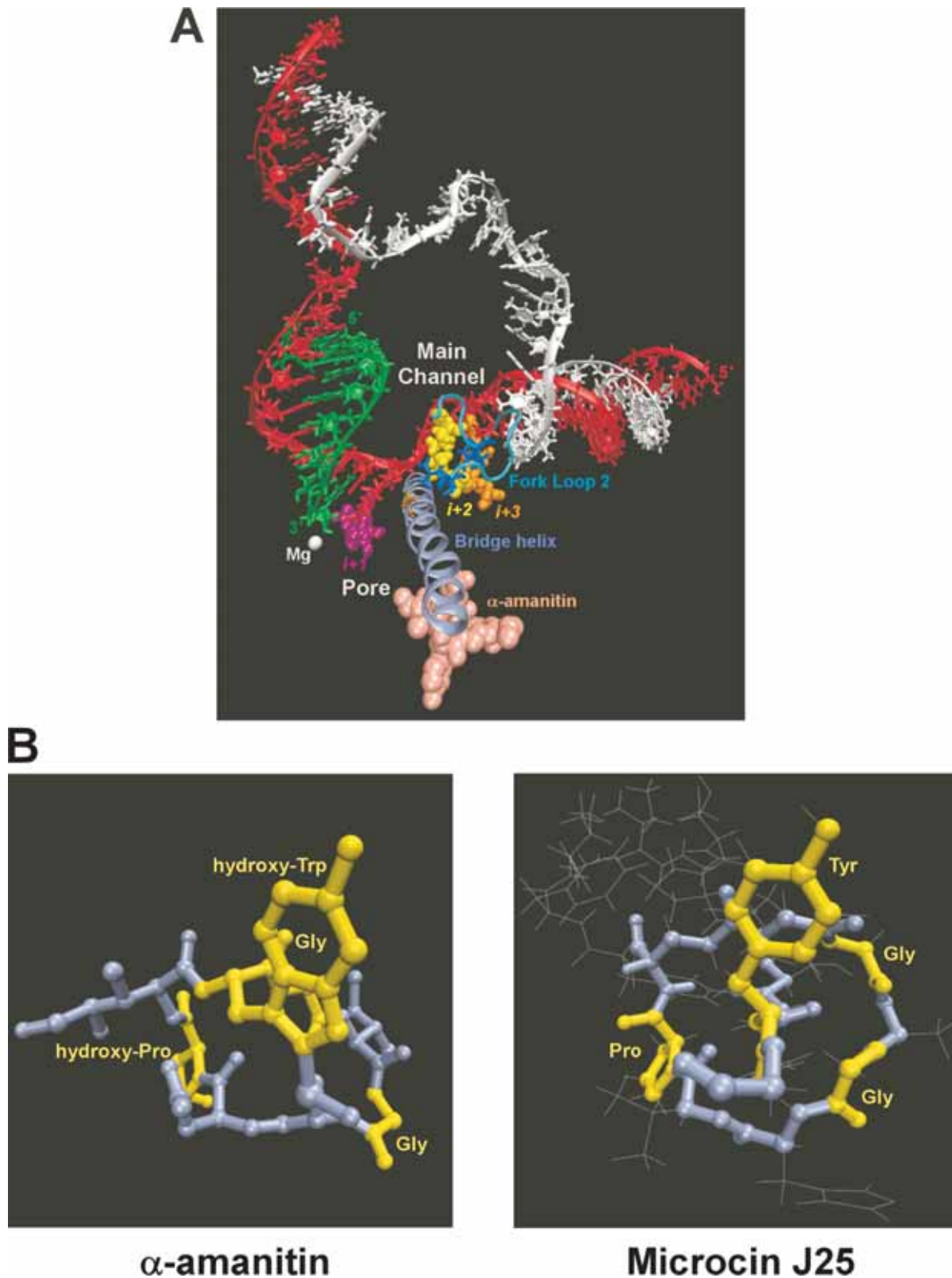
Based on our work and available crystal-structure x-rays, we present a detailed model to describe the preloading of NTP substrates in the RNA polymerase II main channel prior to translocation (Fig. 2). The nontemplate strand is disordered in crystal structures, so its position was modeled in the images (Figs. 2A, 2B). Our model posits 2 NTP- Mg^{2+} substrates ($i+2$ and $i+3$) paired with cognate DNA bases in the main channel; the active site is occupied with another

NTP substrate ($i+1$). We do not believe a third NTP can be accommodated in the main channel because, at the $i+4$ position, an NTP would clash with the nontemplate DNA strand. We posit that main channel NTP substrates help to keep the downstream transcription bubble open, explaining why the bubble can collapse in the absence of appropriate incoming substrates (Kettenberger et al. 2004). For the post-translocated elongation complex, in the presence of substrates, we suggest bubble opening at the $i+2$, $i+3$ and $i+4$ positions, as indicated in the Kornberg structure (Gnatt et al. 2001). To create our model, we placed some amino acids that were disordered in the Kornberg structures (yeast Rpb2 fork loop 2 region, residues Gly503-Leu508) (Figs. 2C, 2D). The $i+2$ and $i+3$ NTPs pair to their main channel template sites. A binding site forms around the NTPs, bordered by Rpb2 subunit fork loop 2 protein side chains. Available amino acids project the expected basic groups (Rpb2 Arg504, Rpb2 Arg512, Rpb1 Lys1102, and Rpb1 Lys1112) and 1 acidic group (Rpb2 Asp505). It is proposed, therefore, that the binding of NTPs in the main channel sculpts and maintains the downstream edge of the transcription bubble.

This model provides a mechanism by which RNA polymerase II can anticipate upcoming transcriptional stalls. As RNA polymerase II approaches a stall, we have observed that the elongation complex enters the paused state more rapidly than can be accommodated by rate constants into and out of the paused state, indicating that RNA polymerase II senses an upcoming stall before the active site is deprived of substrate (Zhang et al. 2003). According to our current model, the downstream DNA template, Rpb2 fork loop 2, and the nontemplate DNA strand encompass the $i+2$ and $i+3$ NTP- Mg^{2+} substrates to regulate the opening of the downstream edge of the transcription bubble. When NTP sub-

⁴Supplementary data for this minireview are available on the Web site or may be purchased from the Depository of Unpublished Data, Document Delivery, CISTI, National Research Council Canada, Ottawa, ON K1A 0S2, Canada. DUD 4006. For more information on obtaining material refer to http://cisti-icist.nrc-cnrc.gc.ca/irm/unpub_e.html.

Fig. 4. α -amanitin blocks translocation. (A) Structural model of α -amanitin (pink) bound to the post-translocation elongation complex with 3 substrate NTPs bound. Colors are the same as those indicated in Fig. 2. (B) Structural comparison of α -amanitin (left panel) and Microcin J25 (right panel) (Bayro et al. 2003; Rosengren et al. 2003; Wilson et al. 2003; Gong et al. 2004). For (B) similar amino acids are yellow.



strates are not available, the downstream bubble tends to collapse, leading to enhanced transcriptional pausing. The binding of elongation factors is also expected to influence the extent of downstream bubble opening and, hence, the frequency of pausing.

As described above, the NTP-Mg²⁺ binding site in the main RNA polymerase II channel is expected to screen incoming NTPs for accurate base pairing, for triphosphate tails, and for 2'- and 3'-hydroxyls on the ribose ring. Our model allows for templating at main channel sites and explains why, during NTP deprivation, the transcription bubble can collapse, as observed in the Cramer structure (Kettenberger et al. 2004). Deprived of the *i*+2 and *i*+3 NTPs, RNA polymerase II might close the downstream bubble as it approaches the stall. We posit that yeast RNA polymerase II amino acids Rpb2 Arg504 and Arg512 (contacting the *i*+2 NTP triphosphate) and Rpb1 Lys1102 and Lys1112 (contacting the *i*+3 NTP triphosphate) are involved in screening triphosphate tails. Rpb2 Asp505 is positioned to scan the 2'-3'-cis diol of the *i*+2 ribose ring. We suggest that this interaction may be mediated by a mobile Mg²⁺ atom. For T7 RNA polymerase, a Mg²⁺ is used in a similar manner to prescreen the 2'-hydroxyl of the incoming NTP substrate in the preinsertion site (Temiakov et al. 2004). For RNA polymerase II, neither the NTP-Mg²⁺ binding pockets at the *i*+2 or *i*+3 positions of the transcription bubble are stable binding sites. NTPs are not expected to loiter in the main channel, but rather to rapidly dock and then advance toward the active site, paired with their cognate DNA base. As the DNA template translocates, another NTP-Mg²⁺ occupies the *i*+3 position. (See supplementary Figs. 1A–1C and supplementary Table I for a summary of predictions based on our model and for evolutionary conservation of relevant protein regions.⁴)

As the *i*+2 NTP-Mg²⁺ is transferred to the *i*+1 active site during translocation, other RNA polymerase II residues become important (Figs. 2C, 2D, and 3). Bridge helix Rpb1 Ala828 is encountered during NTP passage past the bridge α -helix (Nedialkov et al. 2003a). Rpb2 Glu529 is expected to help orient the triphosphate, through charge repulsion, during its passage into the active site. Residues on the bridge α -helix and in the underlying trigger loop (Bar-Nahum et al. 2005) may be involved in the translocation mechanism. Amino acids interacting with the RNA–DNA hybrid are also expected to be important, because mobilizing the hybrid likely facilitates translocation (Holmes and Erie 2003).

Mushrooms and antimicrobials

A deadly mushroom toxin, α -amanitin, blocks translocation by human RNA polymerase II (Bushnell et al. 2002; Gong et al. 2004) (Fig. 4). α -amanitin is structurally similar to a bacterial antibiotic Microcin J25. α -amanitin is a bicyclic, covalently crosslinked, and multiply modified octapeptide (Fig. 4B, left panel). Microcin J25 (with 21 amino acids in total) consists of a cyclic octapeptide (amino acids 1–8) and peptide tail (amino acids 9–21), the C-terminus of which can enter the octapeptide ring to form a bridge reminiscent of the α -amanitin covalent crossbridge (Bayro et al. 2003; Rosengren et al. 2003; Wilson et al. 2003) (Fig. 4B, right panel). α -amanitin is the most potent and spe-

cific known inhibitor of human RNA polymerase II, and Microcin J25 inhibits homologous bacterial RNA polymerases (Yuzenkova et al. 2002). Both toxins penetrate the secondary pore, and α -amanitin interacts strongly and specifically with the bridge α -helix (Bushnell et al. 2002) (Fig. 4A), thought to be important in translocation mechanisms (Gnatt et al. 2001; Vassylyev et al. 2002; Bar-Nahum et al. 2005). Similar to its structural analogue α -amanitin, Microcin J25 most likely inhibits translocation. Suggestions that Microcin J25 blocks NTP loading through the secondary pore to inhibit transcription (Adelman et al. 2004; Mukhopadhyay et al. 2004) are not likely correct. Certainly, the cork-in-bottle model for Microcin J25 action is contrary to the NTP-driven translocation model, which posits an alternate route of NTP entry. This issue will be resolved when transient-state kinetic analyses of Microcin J25 inhibition are reported. Single molecule elongation studies have lacked sufficient resolution to discriminate between an inhibitor that blocks substrate binding and one that blocks translocation (Adelman et al. 2004). As a potent translocation inhibitor, α -amanitin has proven to be an incisive probe with which to unravel the human RNA polymerase II elongation mechanism (Gong et al. 2004, 2005).

Fidelity and efficiency

Why did NTP-driven translocation develop as the dominant mechanism for substrate NTP loading into the active sites of multi-subunit RNA polymerases? The answer relates to the requirement for high fidelity and efficiency of RNA synthesis (Nedialkov et al. 2003a; Zhang and Burton 2004). There lingers a textbook ethic that RNA polymerases lack the separate exonuclease activities of DNA polymerases, because RNA is a throw-away copy of the genetic material, and, therefore, errors in transcription are tolerated. Errors in DNA replication, in contrast, are thought to have a more severe consequence, because lesions can be fixed into genetic material as heritable mutations. Based on kinetic studies of elongation, however, it appears that many RNA polymerases are highly accurate enzymes, perhaps matching the fidelity of DNA polymerases, at least during ongoing synthesis. In that case, how do multi-subunit RNA polymerases maintain high fidelity and efficiency during elongation?

For both DNA and RNA polymerases, high fidelity must be achieved with relatively low-affinity substrate binding, because these enzymes must recognize 4 substrates with different shapes and chemical groups. Accurate base-pairing must provide a primary initial screening of the incoming (d)NTP, but it is also essential to screen for or against the 2'-OH, so that DNA polymerases can exclude ribo-NTPs, and RNA polymerases can exclude deoxy-NTPs. Exclusion of mono- and diphosphates is also important. Recent structural data of simple RNA and DNA polymerases and kinetic studies of multi-subunit RNA polymerases indicate that the screening of substrates begins outside the active site of the enzyme, and that a series of checkpoints must be passed before the substrate tightens into the active site for phosphoryl transfer. Preassessment of the NTP substrate largely precludes replication and transcription errors, with low-energy cost, so DNA and RNA polymerases can achieve high fidelity with relatively low-affinity substrate recognition.

For simple RNA and DNA polymerases (i.e., T7 RNA polymerase and *Bacillus stearothermophilus* large-fragment DNA polymerase I), template preinsertion, (d)NTP preinsertion, and insertion (active site) positions of the dNMP template have been defined (Johnson et al. 2003; Johnson and Beese 2004; Temiakov et al. 2004; Yin and Steitz 2004) (Fig. 1B). Substrate (d)NTPs are known to associate with the (d)NTP preinsertion and insertion (active site) positions. Based on the NTP-driven translocation model for human RNA polymerase II, we suggest that accurate (d)NTP binding may be the route favored to drive the elongation complex between the template preinsertion (pretranslocated) and the (d)NTP preinsertion (post-translocated) sites for some simple polymerases. If this supposition is correct, then simple RNA and DNA polymerases may use a (d)NTP-driven translocation mechanism similar to that used by multi-subunit RNA polymerases. This mechanism would allow 2 low-affinity preassessments of the substrate (d)NTP prior to loading it into the active site: 1 at the template preinsertion site (Johnson et al. 2003; Johnson and Beese 2004); and 1 at the (d)NTP preinsertion site (Temiakov et al. 2004). Transfer from the (d)NTP preinsertion site to the active site requires a protein conformational change before potential (d)NMP misincorporation (Temiakov et al. 2004). Prescreening is an effective fidelity check, because a (d)NTP that is rejected outside the active site cannot result in (d)NMP misincorporation. The template preinsertion site for DNA polymerases is located on the opposite side of the O α -helix (Johnson et al. 2003; Johnson and Beese 2004), far from the active site, so initial preassessment of an incoming dNTP might occur far from the active site. In multi-subunit RNA polymerases, initial NTP preassessment occurs on the opposite side of the bridge α -helix (Nedialkov et al. 2003a; Zhang and Burton 2004; Zhang et al. 2005) (Fig. 2C), far from the active site, suggesting that NTP loading and assessment strategies may be similar for nonhomologous simple and multi-subunit enzymes. T7 RNA polymerase opens the downstream transcription bubble at the N-terminal tip of the O'- α -helix (at Phe644). For T7 RNA polymerase, therefore, only a single template base is available to pair with an NTP substrate. To use NTP-driven translocation requires that an NTP pair with template as soon as its DNA base becomes single stranded, during DNA passage past Phe644 and the O'helix. T7 RNA polymerase has been shown to load NTPs to an NTP preinsertion site prior to a conformational change (open to closed transition involving rotation of the O- α -helix finger domain) that brings the substrate NTP into the insertion (active) site (Temiakov et al. 2004).

Kinetic analyses of RNA-dependent RNA polymerase of poliovirus (in the presence of Mn^{2+}) (Arnold and Cameron 2004; Arnold et al. 2004; Castro et al. 2005) are similar to those for human RNA polymerase II (in the presence of Mg^{2+}) (Nedialkov et al. 2003a; Zhang and Burton 2004). Poliovirus RNA polymerase is a homologue of simple RNA and DNA polymerases. This result leads us to believe that simple enzymes, like multi-subunit enzymes, may use (d)NTP-driven translocation mechanisms.

For multi-subunit RNA polymerases, the NTP substrates are prescreened in the main enzyme channel, which is separated from the active site by the bridge α -helix (Nedialkov et al. 2003a; Zhang and Burton 2004) (Figs. 2C, 2D). The in-

coming NTP is first screened by base-pairing to template at the $i+3$ position. It is screened again at the $i+2$ position. We believe that the 2'-OH of the ribose ring is assessed at the $i+2$ position by Rpb2 Asp505, so dNTPs are normally rejected well outside the RNA polymerase II active site. The space from the main enzyme channel to the active site, which the substrate NTP must traverse in transition from the pre- to the post-translocation position, is constrained, so only accurately paired NTPs can successfully complete the passage (Nedialkov et al. 2003a) (Figs. 2C, 2D, and 3). Once beyond the bridge α -helix, the incoming dNMP-NTP base pair is again challenged during an isomerization step from an open to closed active site (Zhang and Burton 2004; Zhang et al. 2005). This is an induced-fit step, similar to the conversion from the preinsertion (open conformation) to the insertion (closed conformation) site for simple RNA and DNA polymerases (Johnson et al. 2003; Johnson and Beese 2004; Temiakov et al. 2004; Yin and Steitz 2004). In kinetic studies, the open to closed transition is indicated by sequestration of active-site metal ions from EDTA chelation (Zhang and Burton 2004; Zhang et al. 2005). For human RNA polymerase II, the apparently slow bond synthesis step may represent a second induced-fit fidelity check within the active site. If the tightened NTP- Mg^{2+} cannot be appropriately deformed to the catalytically competent state, this would signal an error in substrate loading, inducing reversal of isomerization and NTP release. According to the NTP-driven translocation model, pyrophosphate release (bond completion) is coupled to the next NTP-driven translocation (the following bond initiation). If translocation is blocked (through NMP misincorporation), bond synthesis might be reversed and the inaccurately loaded NTP expelled, providing a fidelity check even after phosphodiester bond formation but prior to pyrophosphate release. Thus, simple DNA and RNA polymerases and multi-subunit RNA polymerases use a complex pathway of (d)NTP prescreening with multiple fidelity checks and an induced-fit step (or steps) prior to bond formation. These enzymes may run a final fidelity check after bond formation but before pyrophosphate release. Release of pyrophosphate results in (essentially) irreversible bond completion.

NTP-driven translocation is efficient because it allows for accurate prealignment, prescreening, and presorting of NTP substrates (Nedialkov et al. 2003a; Zhang and Burton 2004). Furthermore, the end of one bond-addition cycle (pyrophosphate release) is coupled to the beginning of the next (translocation and NTP loading) (Zhang and Burton 2004; Zhang et al. 2005). NTPs load through the main channel. In the NTP-driven translocation model, the secondary pore is the route of pyrophosphate release. Improperly loaded and rejected NTP (or dNTP) substrates also exit through the secondary pore in cases in which they pass prescreening checkpoints. Only when the elongation complex is stalled and ratcheted to the post-translocated position can the secondary pore be a route for substrate NTP loading.

Conclusions

In summary, a new view of translocation mechanisms has been developed, based on kinetic analyses of elongation by human RNA polymerase II. NTP-driven translocation is con-

sistent with available kinetic and structural data, although, in the future, inconsistencies with the Cramer elongation-complex structure will have to be resolved. NTP-driven translocation posits that the RNA polymerase secondary pore is not the only, nor is it the major, route of NTP entry into the elongation complex. NTPs are loaded first in the enzyme main channel. NTP-driven translocation provides a new understanding of fidelity and efficiency, indicating that RNA synthesis is a higher-fidelity reaction than was previously thought. Simple RNA and DNA polymerases may use a shorthand version of (d)NTP-driven translocation, providing multiple fidelity checks of the incoming substrate at a low-energy cost.

Inspection of available RNA polymerase II elongation complex structures suggests that the opening and closing of the downstream transcription bubble is regulated during elongation. We suggest that downstream bubble opening is maintained through NTP-Mg²⁺ loading, and is regulated by transcriptional elongation factors. Downstream bubble collapse is a signal for RNA polymerase to pause transcription. Maintenance of the open bubble configuration is the signal for continued rapid synthesis, and is supported by the weak binding of templated NTP-Mg²⁺ substrates within the main RNA polymerase channel.

Disparate models for elongation will be reconciled using a combination of structural studies, transient-state kinetic analyses, and mutagenic studies. Understanding the coupled mechanisms of translocation and NTP-Mg²⁺ prescreening is important to the understanding of the fidelity and efficiency of multi-subunit RNA polymerases.

Acknowledgements

This work was supported by a grant from the National Institutes of Health (GM57461 to Z.F.B.). Z.F.B. is a recipient of support from the Michigan State University Agricultural Experiment Station and the College of Osteopathic Medicine.

References

- Adelman, K., Yuzenkova, J., La Porta, A., Zenkin, N., Lee, J., Lis, J.T. et al. 2004. Molecular mechanism of transcription inhibition by peptide antibiotic Microcin J25. *Mol. Cell*, **14**: 753–762.
- Arnold, J.J., and Cameron, C.E. 2004. Poliovirus RNA-dependent RNA polymerase (3Dpol): pre-steady-state kinetic analysis of ribonucleotide incorporation in the presence of Mg²⁺. *Biochemistry*, **43**: 5126–5137.
- Arnold, J.J., Gohara, D.W., and Cameron, C.E. 2004. Poliovirus RNA-dependent RNA polymerase (3Dpol): pre-steady-state kinetic analysis of ribonucleotide incorporation in the presence of Mn²⁺. *Biochemistry*, **43**: 5138–5148.
- Bar-Nahum, G., Epshtein, V., Ruckenstein, A.E., Rafikov, R., Mustae, A., and Nudler, E. 2005. A ratchet mechanism of transcription elongation and its control. *Cell*, **120**: 183–193.
- Batada, N.N., Westover, K.D., Bushnell, D.A., Levitt, M., and Kornberg, R.D. 2004. Diffusion of nucleoside triphosphates and role of the entry site to the RNA polymerase II active center. *Proc. Natl. Acad. Sci. U.S.A.* **101**: 17361–17364.
- Bayro, M.J., Mukhopadhyay, J., Swapna, G.V., Huang, J.Y., Ma, L.C., Sineva, E. et al. 2003. Structure of antibacterial peptide Microcin J25: a 21-residue lariat protoknot. *J. Am. Chem. Soc.* **125**: 12382–12383.
- Bushnell, D.A., Cramer, P., and Kornberg, R.D. 2002. Structural basis of transcription: α -amanitin-RNA polymerase II cocrystal at 2.8 Å resolution. *Proc. Natl. Acad. Sci. U.S.A.* **99**: 1218–1222.
- Castro, C., Arnold, J.J., and Cameron, C.E. 2005. Incorporation fidelity of the viral RNA-dependent RNA polymerase: a kinetic, thermodynamic and structural perspective. *Virus Res.* **107**: 141–149.
- Foster, J.E., Holmes, S.F., and Erie, D.A. 2001. Allosteric binding of nucleoside triphosphates to RNA polymerase regulates transcription elongation. *Cell*, **106**: 243–252.
- Gnatt, A.L., Cramer, P., Fu, J., Bushnell, D.A., and Kornberg, R.D. 2001. Structural basis of transcription: an RNA polymerase II elongation complex at 3.3 Å resolution. *Science (Wash. D.C.)*, **292**: 1876–1882.
- Gong, X.Q., Nedialkov, Y.A., and Burton, Z.F. 2004. α -amanitin blocks translocation by human RNA polymerase II. *J. Biol. Chem.* **279**: 27422–27427.
- Gong, X.Q., Zhang, C., Feig, M., and Burton, Z.F. 2005. Dynamic error correction and regulation of downstream bubble opening by human RNA polymerase II. *Mol. Cell*, **18**: 461–470.
- Guajardo, R., and Sousa, R. 1997. A model for the mechanism of polymerase translocation. *J. Mol. Biol.* **265**: 8–19.
- Holmes, S.F., and Erie, D.A. 2003. Downstream DNA sequence effects on transcription elongation. Allosteric binding of nucleoside triphosphates facilitates translocation via a ratchet motion. *J. Biol. Chem.* **278**: 35597–35608.
- Johnson, K.A. 1992. Transient-state kinetic analysis of enzyme reaction pathways. *Enzymes*, **20**: 1–61.
- Johnson, K.A. 1995. Rapid quench kinetic analysis of polymerases, adenosinetriphosphatases, and enzyme intermediates. *Methods Enzymol.* **249**: 38–61.
- Johnson, S.J., and Beese, L.S. 2004. Structures of mismatch replication errors observed in a DNA polymerase. *Cell*, **116**: 803–816.
- Johnson, S.J., Taylor, J.S., and Beese, L.S. 2003. Processive DNA synthesis observed in a polymerase crystal suggests a mechanism for the prevention of frameshift mutations. *Proc. Natl. Acad. Sci. U.S.A.* **100**: 3895–3900.
- Kettenberger, H., Armache, K.J., and Cramer, P. 2004. Complete RNA polymerase II elongation complex structure and its interactions with NTP and TFIIS. *Mol. Cell*, **16**: 955–965.
- Kireeva, M.L., Komissarova, N., Waugh, D.S., and Kashlev, M. 2000. The 8-nucleotide-long RNA:DNA hybrid is a primary stability determinant of the RNA polymerase II elongation complex. *J. Biol. Chem.* **275**: 6530–6536.
- Landick, R. 2004. Active-site dynamics in RNA polymerases. *Cell*, **116**: 351–353.
- Mukhopadhyay, J., Sineva, E., Knight, J., Levy, R.M., and Ebricht, R.H. 2004. Antibacterial peptide Microcin J25 inhibits transcription by binding within and obstructing the RNA polymerase secondary channel. *Mol. Cell*, **14**: 739–751.
- Nedialkov, Y.A., Gong, X.Q., Hovde, S.L., Yamaguchi, Y., Handa, H., Geiger, J.H. et al. 2003a. NTP-driven translocation by human RNA polymerase II. *J. Biol. Chem.* **278**: 18303–18312.
- Nedialkov, Y.A., Gong, X.Q., Yamaguchi, Y., Handa, H., and Burton, Z.F. 2003b. Transient state kinetics of RNA polymerase II elongation. *Methods Enzymol.* **371**: 252–262.
- Oster, G. 2002. Brownian ratchets: Darwin's motors. *Nature (London)*, **417**: 25.
- Patel, S.S., Wong, I., and Johnson, K.A. 1991. Pre-steady-state kinetic analysis of processive DNA replication including complete

- characterization of an exonuclease-deficient mutant. *Biochemistry*, **30**: 511–525.
- Rosengren, K.J., Clark, R.J., Daly, N.L., Goransson, U., Jones, A., and Craik, D.J. 2003. Microcin J25 has a threaded sidechain-to-backbone ring structure and not a head-to-tail cyclized backbone. *J. Am. Chem. Soc.* **125**: 12464–12474.
- Sousa, R. 2003. On models and methods for studying polymerase translocation. *Methods Enzymol.* **371**: 3–13.
- Sousa, R. 2005. Machinations of a maxwellian demon. *Cell*, **120**: 155–156.
- Temiakov, D., Patlan, V., Anikin, M., McAllister, W.T., Yokoyama, S., and Vassylyev, D.G. 2004. Structural basis for substrate selection by T7 RNA polymerase. *Cell*, **116**: 381–391.
- Vassylyev, D.G., Sekine, S., Laptenko, O., Lee, J., Vassylyeva, M.N., Borukhov, S., and Yokoyama, S. 2002. Crystal structure of a bacterial RNA polymerase holoenzyme at 2.6 Å resolution. *Nature (London)*, **417**: 712–719.
- Wang, H., and Oster, G. 2002. Ratchets, power strokes, and molecular motors. *Appl. Phys. A* **75**: 315–323.
- Westover, K.D., Bushnell, D.A., and Kornberg, R.D. 2004a. Structural basis of transcription: separation of RNA from DNA by RNA polymerase II. *Science (Wash. D.C.)*, **303**: 1014–1016.
- Westover, K.D., Bushnell, D.A., and Kornberg, R.D. 2004b. Structural basis of transcription; nucleotide selection by rotation in the RNA polymerase II active center. *Cell*, **119**: 481–489.
- Wilson, K.A., Kalkum, M., Ottesen, J., Yuzenkova, J., Chait, B.T., Landick, R. et al. 2003. Structure of Microcin J25, a peptide inhibitor of bacterial RNA polymerase, is a lassoed tail. *J. Am. Chem. Soc.* **125**: 12475–12483.
- Yin, Y.W., and Steitz, T.A. 2002. Structural basis for the transition from initiation to elongation transcription in T7 RNA polymerase. *Science (Wash. D.C.)*, **298**: 1387–1395.
- Yin, Y.W., and Steitz, T.A. 2004. The structural mechanism of translocation and helicase activity in T7 RNA polymerase. *Cell*, **116**: 393–404.
- Yuzenkova, J., Delgado, M., Nechaev, S., Savalia, D., Epshtein, V., Artsimovitch, I. et al. 2002. Mutations of bacterial RNA polymerase leading to resistance to Microcin J25. *J. Biol. Chem.* **277**: 50867–50875.
- Zhang, C., and Burton, Z.F. 2004. Transcription factors IIF and IIS and nucleoside triphosphate substrates as dynamic probes of the human RNA polymerase II mechanism. *J. Mol. Biol.* **342**: 1085–1099.
- Zhang, C., Yan, H., and Burton, Z.F. 2003. Combinatorial control of human RNA polymerase II (RNAP II) pausing and transcript cleavage by transcription factor IIF, hepatitis δ antigen, and stimulatory factor II. *J. Biol. Chem.* **278**: 50101–50111.
- Zhang, C., Zobeck, K.L., and Burton, Z.F. 2005. Human RNA polymerase II elongation in slow motion: role of the TFIIF RAP74 α 1 helix in NTP-driven translocation. *Mol. Cell. Biol.* **25**: 3583–3595.